

Stratification Instability in Granular Flows

Hernán A. Makse

*Laboratoire de Physique de la Matière Condensée, Collège de France
11 place Marcelin Berthelot, 75231 Paris Cedex 05, France*
and

Center for Polymer Studies, and Physics Dept., Boston University, Boston, MA 02215 USA
(Phys. Rev. E, **56**, 7008-7016 (1997))

When a mixture of two kinds of grains differing in size and shape is poured in a vertical two-dimensional cell, the mixture spontaneously stratifies in alternating layers of small and large grains, whenever the large grains are more faceted than the small grains. Otherwise, the mixture spontaneously segregates in different regions of the cell when the large grains are more rounded than the small grains. We address the question of the origin of the instability mechanism leading to stratification using a recently proposed set of equations for surface flow of granular mixtures. We show that the stable solution of the system is a segregation solution due to size (large grains tend to segregate downhill near the substrate and small grains tend to segregate uphill) and shape (rounded grains tend to segregate downhill and more faceted grains tend to segregate uphill). As a result, the segregation solution of the system is realized for mixtures of large-rounded grains and small-cubic grains with the large-rounded grains segregating near the bottom of the pile. Stability analysis reveals the instability mechanism driving the system to stratification as a competition between size-segregation and shape-segregation taking place for mixtures of large-cubic grains and small-rounded grains. The large-cubic grains tend to size-segregate at the bottom of the pile, while at the same time, they tend to shape-segregate near the pouring point. Thus, the segregation solution becomes unstable, and the system evolves spontaneously to stratification.

I. INTRODUCTION

One of the unusual properties [1,2] of granular materials [3–8] is the size-segregation of mixtures when they are exposed to external periodic perturbations such as vibrations or rotations [9–15]. Size-segregation also occurs when a mixture of grains of different size is simply poured onto a heap [16–21]: the large grains spontaneously segregate near the bottom of the heap, whereas the small grains segregate near the pouring point at the top of the heap.

Recently, it was shown [22] that when a mixture composed of grains differing not only in size but also in shape is poured in a “granular Hele-Shaw cell” (two vertical slabs separated by a gap ≈ 5 mm), a spontaneous stratification is observed. Granular mixtures of small-rounded grains and large-cubic grains stratify in alternating layers of small-rounded and large-cubic grains parallel to the surface of the pile when they are poured in the cell.

According to the experiments [22], the control parameter for stratification appears to be the difference of the repose angles of the pure species

$$\delta \equiv \theta_{22} - \theta_{11}, \quad (1)$$

where θ_{11} is the angle of repose of the small grains, and θ_{22} is the angle of repose of the large grains. The stratification experiments [22] used a mixture of grains of different shapes (small rounded or less faceted grains and large cubic or more faceted grains). The repose angle of the smaller pure species is then smaller than the repose angle of the large pure species—i.e., $\delta > 0$. On the other hand, strong segregation but not stratification occurred

[22] when $\delta < 0$, (corresponding to a mixture of small-cubic grains, and large-rounded grains) [23]. We notice that the angle of repose of the pure species does not depend on the size of the grains, and it is a function of the shape of the grains: the rougher the grains the larger the angle of repose.

To describe the case of a single-species sandpile in a two-dimensional geometry, Bouchaud, Cates, R. Prakash, and Edwards (BCRE) [26,27] developed a novel theoretical approach. They introduced two coarse-grained variables: the local height of the sandpile, and the local “thickness” of the layer of rolling grains, and a set of coupled equations to govern the flow of the rolling grains and their interaction with the sandpile. Recently, de Gennes [28] applied the BCRE formalism to the case of granular flows in a thin rotating drum [29,30], and very recently Boutreux and de Gennes (BdG) [31] treated the case of granular flows made of two species of different angles of repose. Makse, Cizeau and Stanley (MCS) [32,33] reproduced stratification and segregation using a discrete model and the continuum approach developed by BdG. They showed that a “kink” mechanism [32,33] describes the dynamics of stratification in agreement with experimental findings [22].

In this paper, we address the question of the origin of the instability leading to stratification. We study analytically segregation and stratification as observed in [22] when the two species have different size and different shape (or, in general, different angle of repose) [34]. We use the continuum approach of BdG [31], and MCS [32,33], to calculate the steady-state solution of the equations of motion for surface flow of granular mixtures. This solution shows the complete size-segregation of the

mixture with the large grains being found at the bottom of the pile. We then study analytically the conditions under which the instability leading to stratification occurs. Stability analysis shows that the steady-state solution is stable under perturbations only when $\delta < 0$, while the segregation solution is unstable (leading to stratification) when $\delta > 0$, in agreement with experiments [22].

The stratification instability can be seen as follows. There are two segregation mechanisms acting when pouring a mixture of grains differing in size and shape in a cell:

- **Size-segregation:** large grains tend to segregate downhill near the bottom of the pile, and small grains tend to segregate uphill near the pouring point, since large grains roll down easier on top of small grains than small grains on top of large grains (Fig. 1a).
- **Shape-segregation:** cubic grains tend to segregate near top of the pile, and rounded grains segregate near the bottom, since rounded grains roll down easier than cubic grains (Fig. 1b).

Thus, when pouring a mixture of small-cubic grains and large-rounded grains the segregation of the mixture results, since the small-cubic grains size-segregate and shape-segregate near the top of the pile, and the large-rounded grains size and shape-segregate near the bottom. This situation gives rise to the steady-state solution of the system.

On the other hand, the stratification process arises as a consequence of an instability mechanism. For mixtures of large-cubic grains and small-rounded grains there exists a competition between size-segregation and shape-segregation. Large-cubic grains tend to size-segregate at the bottom of the pile, while at the same time, they tend to shape-segregate at the top of the pile. Thus, the segregation solution becomes unstable, and the instability drives the system spontaneously to stratification.

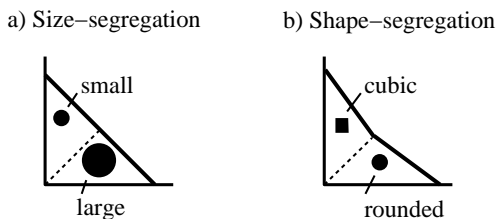


FIG. 1. Two segregation effects acting when the grains differ in size and shape. **a**, Size-segregation: large grains tend to segregate at the bottom of the pile. **b**, Shape-segregation: rounded grains tend to segregate at the bottom of the pile.

In the following we take up each of these results in turn. The paper is organized as follows: In Section II we present the theoretical formalism for surface flows of

granular mixtures. In Section III we calculate the steady-state solution of the problem. In Section IV we perform a stability analysis, and in Section V we discuss the instability mechanism for stratification and we propose a phase diagram for surface flows of granular mixtures in light of these results.

II. THEORY FOR SURFACE FLOW OF GRANULAR MIXTURES

The theoretical study of surface flows of granular materials was triggered by the works of BCRE [26,27] and Mehta and collaborators [36]. In a recent theoretical study for the case of a single-species sandpile BCRE [26,27] proposed two coupled variables to describe the dynamics of two-dimensional sandpile surfaces: the local angle of the sandpile $\theta(x, t)$ (or alternatively the height of the sandpile $h(x, t)$) which describes the static phase (i.e., the grains which belong to the pile), and the local thickness of the layer of rolling grains $R(x, t)$ to describe the rolling phase (i.e., the grains that are not part of the pile but roll downwards on top of the static phase). BCRE also proposed a set of convective-diffusion equation for the rolling grains, which was later simplified by de Gennes [28]:

$$\frac{\partial R(x, t)}{\partial t} = -v \frac{\partial R}{\partial x} + \Gamma(R, \theta), \quad (2)$$

where v is the downhill drift velocity of the grains along x , assumed to be constant in space and in time. The interaction term Γ takes into account the conversion of static grains into rolling grains, and vice versa. The simplest form of Γ is [26–28]

$$\Gamma(R, \theta) = \gamma (\theta(x, t) - \theta_r) R(x, t). \quad (3)$$

Here θ_r denotes the angle of repose (the maximum angle below which a rolling grain is converted into a static grain [26,27,37,38]). The rate $\gamma > 0$ has dimension of inverse time, and v/γ represents the length scale at which a rolling grain will interact significantly with a surface at an angle slightly above or below the angle of repose [28]. For notational convenience we do not consider the difference between the angle and the tangent of the angle, i.e.

$$\theta(x, t) \equiv -\frac{\partial h}{\partial x}. \quad (4)$$

The equation for $h(x, t)$ follows by conservation

$$\frac{\partial h(x, t)}{\partial t} = -\Gamma(R, \theta). \quad (5)$$

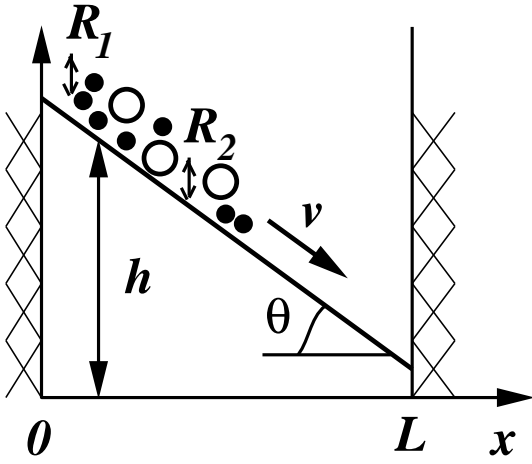


FIG. 2. Diagram showing the variables used to describe the granular flow of mixtures in a granular Hele-Shaw cell or two-dimensional silo.

Recently, BdG [31] have extended the BCRE formalism to the case of two species. This formalism considers the two local “equivalent thicknesses” of the species in the rolling phase $R_\alpha(x, t)$ (i.e. the total thickness of the rolling phase multiplied by the local volume fraction of the α grains in the rolling phase at position x), with $\alpha = 1, 2$ respectively for small and large grains. The total thickness of the rolling phase is defined as

$$R(x, t) \equiv R_1(x, t) + R_2(x, t). \quad (6)$$

The static phase is described by the height of the sandpile $h(x, t)$, and the volume fraction of static grains $\phi_\alpha(x, t)$ of type α at the surface of the pile. Here x is the longitudinal coordinate, and the pouring point is assumed to be at $x = 0$, and we consider a silo or cell of lateral size L (see Fig. 2).

The equations of motion for the rolling species are [31]

$$\frac{\partial R_\alpha(x, t)}{\partial t} = -v_\alpha \frac{\partial R_\alpha}{\partial x} + \Gamma_\alpha, \quad (7a)$$

and the equation for $h(x, t)$ follows by conservation

$$\frac{\partial h(x, t)}{\partial t} = -\Gamma_1 - \Gamma_2. \quad (7b)$$

Here v_α is the downhill convection velocity of species α along x . The interaction term Γ_α takes into account the conversion of rolling grains of type α into static grains, and the amplification of static grains α by rolling grains of type α or β . Γ_α is defined through a 2×2 collision matrix $M_{\alpha\beta}$

$$\Gamma_\alpha(\theta, R_\alpha, \phi_\alpha) \equiv \sum_{\beta=1}^2 M_{\alpha\beta} R_\beta. \quad (7c)$$

The elements of the collision matrix $M_{\alpha\beta}$ characterize the interaction of a rolling grain of type β with a surface of static grains of type α , and they are determined by the local angle $\theta(x, t)$, and the concentrations $\phi_\alpha(x, t)$. The concentrations of static grains at the surface of the pile $\phi_\alpha(x, t)$ are given by

$$\phi_\alpha(x, t) \frac{\partial h}{\partial t} = -\Gamma_\alpha, \quad (7d)$$

and

$$\phi_1 + \phi_2 = 1. \quad (7e)$$

The *canonical* form of the collision matrix is defined by taking into account a set of binary collisions between a rolling and a static grains [31,39]

$$\hat{M} \equiv \begin{vmatrix} a_1(\theta)\phi_1 - b_1(\theta) & x_2(\theta)\phi_1 \\ x_1(\theta)\phi_2 & a_2(\theta)\phi_2 - b_2(\theta) \end{vmatrix} \quad (8)$$

This definition involves a set of a priori unknown collision functions contributing to the rate processes: $a_\alpha(\theta)$ is the contribution due to an amplification process, (i.e., when a static grain of type α is converted into a rolling grain due to a collision by a rolling grain of type α), $b_\alpha(\theta)$ is the contribution due to capture of a rolling grain of type α , (i.e., when a rolling grain of type α is converted into a static grain), and $x_\alpha(\theta)$ is the contribution due to a cross-amplification process, (i.e., the amplification of a static grain of type β due to a collision by a rolling grain of type α).

BdG [31] used a “minimal” form of the collision matrix to calculate the steady-state solution in the geometry of a two-dimensional silo for the case of mixtures of grains differing only in angle of repose. This solution shows a complete segregation at the low edge of the silo, and near this point the concentrations of static grains show power-law behavior. In their model, they consider a constant cross-amplification term $x_\alpha(\theta) = \text{const}$, and they consider the angle of repose of each species to be independent on the surface composition of the pile. A generalization of the minimal model of [31] to include not only different surface properties of the species but also different size of the species with small size ratios ($d_2/d_1 < 1.4$) is considered in [35].

Here, we use the BdG equations to study segregation as well as stratification of mixtures of grains differing in size and shape in a two-dimensional silo (Fig. 2). As in MCS [32], we focus on the dependence of the repose angle of every species on the composition of the surface $\phi_\beta(x, t)$. We use the following definitions of collision functions [32]:

$$\begin{aligned} a_\alpha(\theta) &\equiv \gamma_{\alpha\alpha} \Pi[\theta(x, t) - \theta_\alpha(\phi_\beta)] \\ b_\alpha(\theta) &\equiv \gamma_{\alpha\alpha} \Pi[\theta_\alpha(\phi_\beta) - \theta(x, t)] \\ x_\beta(\theta) &\equiv \gamma_{\beta\alpha} \Pi[\theta(x, t) - \theta_\beta(\phi_\beta)], \end{aligned} \quad (9a)$$

where

$$\Pi[x] \equiv \begin{cases} 0 & \text{if } x < 0 \\ x & \text{if } x \geq 0 \end{cases}. \quad (9b)$$

Here, the rates are $\gamma_{\alpha\alpha} > 0$, and the generalized angle of repose $\theta_\alpha(\phi_\beta)$ of a α type of rolling grain is a continuous function of the composition of the surface ϕ_β [32] (see Fig. 3, where we also define $\theta_{\alpha\beta}$ as $\theta_\alpha(\phi_\beta)$ for $\phi_\beta = 1$):

$$\begin{aligned}\theta_1(\phi_2) &= m\phi_2 + \theta_{11} \\ \theta_2(\phi_2) &= m\phi_2 + \theta_{21} = -m\phi_1 + \theta_{22},\end{aligned}\quad (10)$$

where $m \equiv \theta_{12} - \theta_{11} = \theta_{22} - \theta_{21}$. We have assumed the difference

$$\psi \equiv \theta_1(\phi_2) - \theta_2(\phi_2) \quad (11)$$

to be independent of the concentration ϕ_2 . We notice that the fact that grains 1 are smaller than grains 2 implies $\theta_1(\phi_2) > \theta_2(\phi_2)$ for any given concentration ϕ_2 (i.e. the small grains are always the first to be captured). The angular difference ψ is thus determined by the difference in size between the grains; the larger the size difference the larger ψ . Moreover, the fact that the grains have different shapes implies $\theta_{11} \neq \theta_{22}$, (for instance $\theta_{11} < \theta_{22}$ when the grains 1 are more rounded than the grains 2).

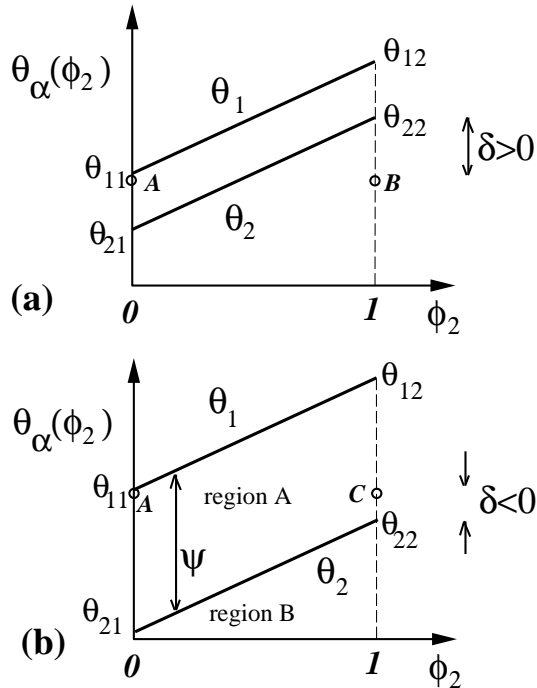


FIG. 3. Dependence of the generalized angle of repose for the two types of rolling grains on the concentration of the surface of large grains ϕ_2 for **a**, $\delta > 0$, and **b**, $\delta < 0$, where δ is defined in Eq. (1). We define $\theta_{\alpha\beta} = \theta_\alpha(\phi_\beta = 1)$ [32].

The collision matrix includes the following processes [31] (Fig. 4).

(a) *Capture*, $b_\alpha(\theta)$: rolling grains are captured if the local angle of the sandpile $\theta(x, t)$ is smaller than the generalized repose angle $\theta_\alpha(\phi_\beta)$. The capture is proportional to R_α [40].

(b) *Amplification*, $a_\alpha(\theta)$: if the local angle $\theta(x, t)$ is larger than the generalized repose angle $\theta_\alpha(\phi_\beta)$, then some static grains of type α will be converted into rolling grains due to a collision by rolling grains of type α . The amplification rate is proportional to the concentration ϕ_α in the sandpile, and to R_α .

(c) *Cross-amplification*, $x_\alpha(\theta)$: when static grains of type α are amplified by rolling grains of type β . This cross-amplification occurs when the local angle $\theta(x, t)$ is larger than $\theta_\beta(\phi_\beta)$.

Equation (7a) now reads

$$\begin{aligned}\frac{\partial R_\alpha}{\partial t} &= -v_\alpha \frac{\partial R_\alpha}{\partial x} + \gamma_{\alpha\alpha} \Pi[\theta(x, t) - \theta_\alpha(\phi_\beta)] \phi_\alpha R_\alpha \\ &\quad - \gamma_{\alpha\alpha} \Pi[\theta_\alpha(\phi_\beta) - \theta(x, t)] R_\alpha \\ &\quad + \gamma_{\beta\alpha} \Pi[\theta(x, t) - \theta_\beta(\phi_\beta)] \phi_\alpha R_\beta\end{aligned}\quad (12)$$

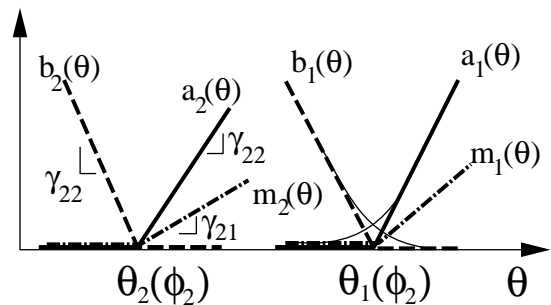


FIG. 4. Schematic plot of capture $b_\alpha(\theta)$, amplification $a_\alpha(\theta)$, and cross-amplification $x_\alpha(\theta)$ functions used in the definition of the present model. These functions are expected to be continuous in a region near the angle of repose (as shown by the thin curves). However, when the ratio between the size of the grains is not close to one, then $\psi = \theta_1(\phi_2) - \theta_2(\phi_2)$ is large enough so we can approximate these functions by the forms shown in this figure.

III. STEADY-STATE SOLUTION.

We now calculate the steady-state solution of the equations of motion for the two-species sandpile including the terms corresponding to cross-amplification $M_{\alpha\beta}$, $\alpha \neq \beta$, which were not considered in [32].

We consider the geometry of a silo of lateral size L (Fig. 2). We assume that the difference $\psi = \theta_1(\phi_2) - \theta_2(\phi_2)$ is independent of the concentration ϕ_2 , then $\psi = \theta_{11} - \theta_{21} = \theta_{12} - \theta_{22}$ (see Fig. 3). We set $v_1 = v_2 \equiv v$, and $\gamma_{11} = \gamma_{22} = \gamma$, and we keep $\gamma_{12} \neq \gamma_{21}$. We seek a solution where the profiles of the sandpile and of the rolling grains do not change in time. Since stratification is an oscillatory solution, stratification cannot be observed for the steady-state solution. We set

$$\frac{\partial h}{\partial t} = v \frac{R^0}{L}, \quad (13a)$$

and

$$\frac{\partial R_\alpha(x)}{\partial t} = 0, \quad (13b)$$

with boundary conditions $R_\alpha(x=0) = R_\alpha^0$, and $R_\alpha(x=L) = 0$, and $R^0 \equiv R_1^0 + R_2^0$.

We first calculate the profile of the total rolling species $R(x) = R_1(x) + R_2(x)$. From (7a), (7b), and (13) we obtain

$$0 = \frac{\partial R(x)}{\partial t} = -v \frac{\partial R(x)}{\partial x} - v \frac{R^0}{L}, \quad (14)$$

so that the profile of total rolling species decays linearly with x ,

$$R(x) = \frac{R^0}{L}(L - x). \quad (15)$$

From (7d), (12), and (13a) we obtain the concentrations

$$\phi_1(x) = \frac{\gamma \Pi[\theta_1(\phi_2) - \theta(x)] R_1(x)}{vR^0/L + \gamma\Pi[\theta - \theta_1]R_1(x) + \gamma_{21}\Pi[\theta - \theta_2]R_2(x)}, \quad (16a)$$

$$\phi_2(x) = \frac{\gamma \Pi[\theta_2(\phi_2) - \theta(x)] R_2(x)}{vR^0/L + \gamma\Pi[\theta - \theta_2]R_2(x) + \gamma_{12}\Pi[\theta - \theta_1]R_1(x)}. \quad (16b)$$

The equations for the rolling species are obtained from (7a), (7d), and (13),

$$v \frac{\partial R_\alpha(x)}{\partial x} = -(vR^0/L) \phi_\alpha(x), \quad (17)$$

Next, we divide the calculations in two regions: Region A, where $\theta_2(\phi_2) < \theta < \theta_1(\phi_2)$, and Region B, where $\theta < \theta_2(\phi_2) < \theta_1(\phi_2)$ (see Fig. 3b). The steady-state solution of Eqs. (7) and (9) shows a strong segregation pattern.

Region A. At the upper part of the pile we find that only small grains are present (for $0 \leq x \leq x_m$, with $x_m = R_1^0 L / R^0 - v / (\gamma\psi)$, see below).

If $\theta_2 < \theta < \theta_1$, from (16) we obtain [41]

$$\phi_1(x) = 1, \quad \phi_2(x) = 0. \quad (18)$$

Using (17) and (18) we find the profiles of the rolling species

$$R_1(x) = R_1^0 - \frac{R^0}{L}x, \quad R_2(x) = R_2^0. \quad (19)$$

The profile of the sandpile is obtained from (7b), (12), and (13a)

$$-\frac{vR^0}{L} = \gamma(\theta(x) - \theta_{11})R_1(x) + \gamma_{21}(\theta(x) - \theta_{21})R_2(x), \quad (20)$$

so that

$$\theta(x) - \theta_{11} = \frac{-v/\gamma - \psi\gamma_{21}LR_2^0/(\gamma R^0)}{L(R_1^0 + R_2^0\gamma_{21}/\gamma)/R^0 - x}. \quad (21)$$

This solution is valid when $\theta(x) > \theta_1(\phi_2 = 1) = \theta_{21}$. Then it is valid for $x < x_m$, where x_m is

$$x_m = \frac{R_1^0}{R^0}L - \frac{v}{\gamma\psi}. \quad (22)$$

Region B. At the lower part of the pile ($x_m \leq x \leq L$), we find that, after a small region of the order of $v/(\gamma\psi)$, mainly large grains are present.

If $\theta < \theta_2 < \theta_1$, from (7b), (12), and (13a) we obtain

$$-\frac{vR^0}{\gamma L} = [\theta(x) - \theta_1(\phi_2)]R_1(x) + [\theta(x) - \theta_2(\phi_2)]R_2(x), \quad (23)$$

and therefore

$$\theta(x) - \theta_2(\phi_2) = \frac{-vR^0/(\gamma L) + \psi R_1(x)}{R(x)}. \quad (24)$$

Inserting (24) in (16) we obtain the concentrations as a function of the rolling species

$$\phi_1(x) = \frac{R_1(x)}{R(x)} \left(1 + \frac{\gamma\psi L}{vR^0} R_2(x) \right), \quad (25a)$$

$$\phi_2(x) = \frac{R_2(x)}{R(x)} \left(1 - \frac{\gamma\psi L}{vR^0} R_1(x) \right). \quad (25b)$$

We obtain the equations for the rolling species using Eqs. (17) and (25),

$$\frac{\partial R_1(x)}{\partial x} = -\frac{R_1(x)}{R(x)} \left(\frac{R^0}{L} + \frac{R_2(x)}{r} \right), \quad (26a)$$

$$\frac{\partial R_2(x)}{\partial x} = -\frac{R_2(x)}{R(x)} \left(\frac{R^0}{L} - \frac{R_1(x)}{r} \right), \quad (26b)$$

where $r \equiv v/(\gamma\psi)$. Setting $u = R_1/R$ we obtain from (26a)

$$ru' = -(1-u)u, \quad (27)$$

and the solution is

$$\frac{R_1(x)}{R(x)} = \frac{1}{1 + C \exp[(x - x_m)/r]}, \quad (28)$$

where C is an integration constant. By considering the continuity at $x = x_m$, we obtain $C = R_2^0 L / (R^0 r)$ [42]. The profile of the pile is obtained from (24) and (10)

$$\theta(x) - \theta_{22} = -m\phi_1(x) + \frac{\psi R_1(x)L/R^0 - v/\gamma}{(L-x)}. \quad (29)$$

We notice that the parameter $r = v/(\gamma\psi)$ is expected to be of the order of the size of the grains, so for large system size $r \ll L$, and $C \gg 1$. Then the steady-state solution can be simplified, and we arrive to the following simpler forms when also considering that, as in the experiment, an equal volume mixture is used (i.e., $R_1^0 = R_2^0 = R^0/2$).

Region A. Valid for $0 \leq x \leq x_m = L/2 - v/(\gamma\psi)$.

$$\phi_1(x) = 1 \quad \phi_2(x) = 0 \quad (30a)$$

$$R_1(x) = R^0\left(\frac{1}{2} - \frac{x}{L}\right) \quad R_2(x) = \frac{R^0}{2} \quad (30b)$$

$$\theta(x) - \theta_{11} = \frac{-v/\gamma - \psi\gamma_{21}L/(2\gamma)}{(L/2)(1 + \gamma_{21}/\gamma) - x}. \quad (30c)$$

Region B. Valid $x_m \leq x \leq L$.

$$\phi_1(x) = \exp\left[-\frac{\gamma\psi}{v}(x - x_m)\right] \quad (31a)$$

$$R_1(x) = \frac{2v}{\gamma\psi L}\phi_1(x)R(x) \quad (31b)$$

$$\theta(x) - \theta_{22} = -m\phi_1(x) - \frac{v}{\gamma(L-x)}. \quad (31c)$$

Figure 5 shows the profiles of the steady state solution for typical experimental values. We use a cell of size $L = 30$ cm. In [25] the values of the different phenomenological coefficients appearing in the theory were measured for a typical equal-volume mixture consisting of quasi-spherical glass beads of mean diameter 0.27 mm, and cubic-shaped sugar grains of typical size 0.8 mm.

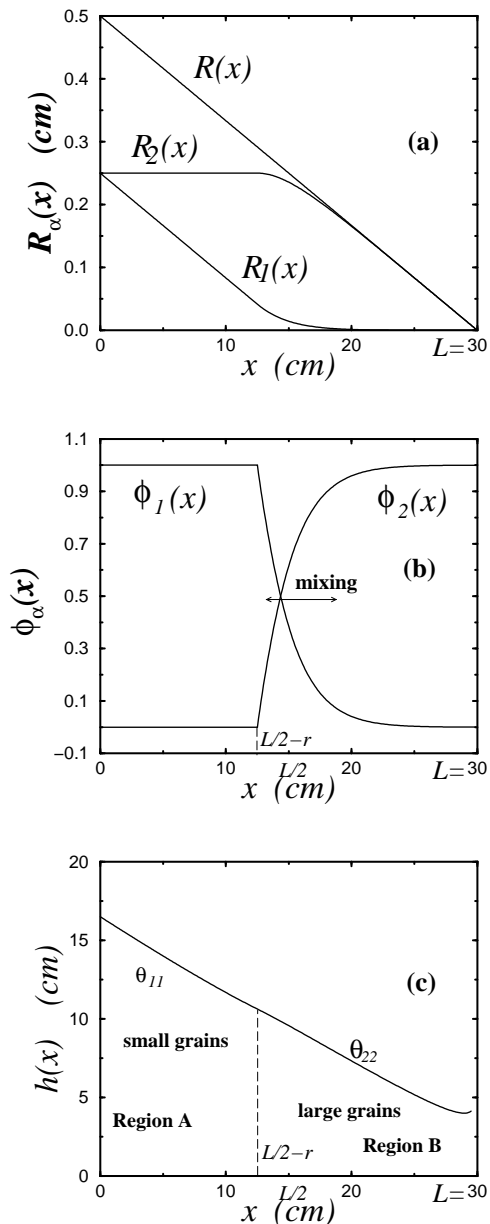


FIG. 5. Steady-state solution (30)–(31) for the two-species granular flow in a silo geometry. We use the following typical experimental values for the phenomenological constants appearing in the theory [44]: $L = 30$ cm, $\tan\theta_{11} = 0.6$, $\tan\theta_{22} = 0.5$, $\tan\psi = 0.2$, $\tan m = 0.1$, $\tan\delta = -0.1$, $R^0 = 0.25$ cm, $v = 10$ cm/sec, $\gamma = 20$ /sec, and $\gamma_{21} = 10$ /sec. **a**, Profiles of the rolling species. **b**, Profile of the concentrations. **c**, Profile of the sandpile.

The mean value of the velocity of the grains falling down the slope is of the order $v \simeq 10$ cm/sec. The rate γ was also estimated in [25] to be of the order of $\gamma \simeq 20$ /sec. A typical value of the thickness of the layer of rolling grains is $R^0 \simeq 0.25$ cm [43]. The difference $\tan\psi = \tan\theta_{11} - \tan\theta_{21}$ is of the order of 0.1 – 0.3 [44]. The concentrations (Fig. 5b) show the strong segregation of the mixture; the mixing of the species is concentrated

only in a small region, of the order of $v/(\gamma \tan \psi) \simeq 1.5-5$ cm, in the center of the pile. The top part of the pile is made of small grains so that the angle is approximately equal to θ_{11} (Fig. 5c). Towards the center of the pile the angle decreases and it is equal to θ_{21} at $x = x_m$ (θ_{21} is the angle at which large grains start to be captured on top of small grains). Then the angle increases gradually to θ_{22} towards the lower part of the pile made of large grains. The profile of $R(x)$ (Fig. 5a) behaves linearly with x , which is a result of the conservation of number of grains Eq. (13a). Same dependence is observed in the case of a single-species sandpile [28]. The exponential behavior of the concentrations and rolling species $R_\alpha(x)$ near the center of the pile is expected, since we are solving equations of the type $\partial R_\alpha/\partial x \sim -(\gamma\psi/v)R_\alpha(x)$. We notice that the segregation solution (30)-(31) is determined by the fact that $\theta_1(\phi_2) > \theta_2(\phi_2)$, i.e. by the fact that the small grains are trapped first since they have a larger generalized angle of repose for a given concentration ϕ_2 . Then, this solution shows the size-segregation of the mixture.

IV. STABILITY ANALYSIS

In the experiments of [22], it was found that there is a transient regime of segregation before the layers appear. The initial segregation regime turns into stratification only for mixtures with $\delta > 0$ (Eq. (1)). At the onset of the instability leading to stratification, it is observed that a small amount of large grains is captured on top of the region of small grains near the center of the pile (Region A, see Fig. 6a). This leads to the appearance of the first layer of larger grains and then to the oscillations characteristic of stratification. On the other hand, if $\theta_{11} > \theta_{22}$ ($\delta < 0$) the segregation profile remains stable (Fig. 6b). This picture was also confirmed by the models proposed in [32].

The first sublayer of large grains corresponds to the appearance of the first “kink” [32,33]. The kink is an uphill wave at which the rolling grains are stopped. This first “kink” is formed only of large grains (as was observed in [22] and [32]). This kink appears to move uphill and creates an incipient layer of large grains. Then the newly arriving grains roll down to the bottom of the pile where a new kink is developed. At this point, the kink (formed by large and small grains) starts to move upwards and all grains are stopped at the kink, but the small-rounded grains are stopped first so that the result is a pair of layers with the small-rounded grains being found underneath the large-cubic grains.

Next, we analyze the stability of the steady-state solution under perturbations, by assuming that the steady-state solution obtained in Section III is valid for the initial transient regime of the evolution. We perturb the steady-state profiles by considering that a small amount of large grains has been captured in the region A, near

the center of the pile ($x \lesssim x_m$), without changing the angle of the pile. We then analyze the short-time evolution of this perturbation to the steady-state profile. The dynamical evolution of the additional large rolling grains are now governed by the following equation:

$$\frac{\partial R_2(x,t)}{\partial t} = -v \frac{\partial R_2}{\partial x} + \gamma(\theta - \theta_{22})R_2, \quad (32)$$

where the repose angle of the large rolling grains is θ_{22} since the surface is made only of large grains.

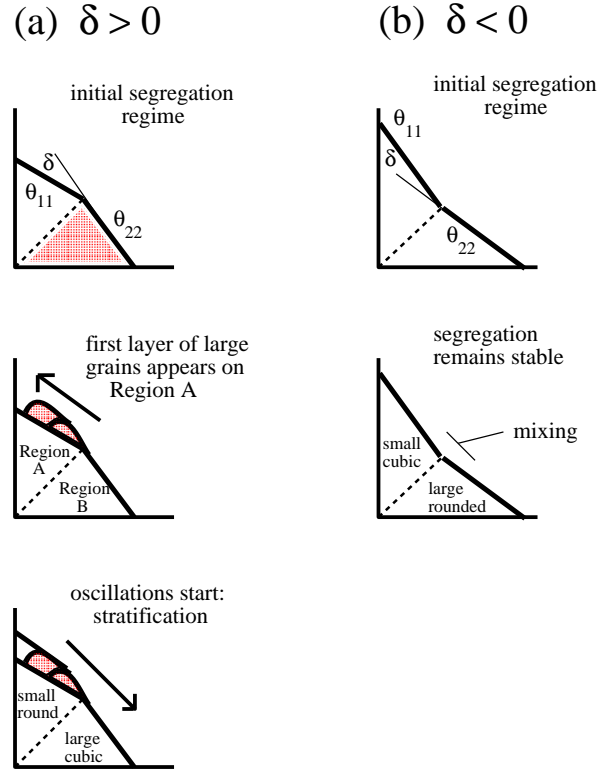


FIG. 6. Schematic process leading to **a**, stratification ($\delta > 0$), and **b**, segregation ($\delta < 0$).

We are interested in the behavior of the profiles near the center of the pile, where R_1 is very small, so we can focus only on the behavior of the large grains. We look for the short-time behavior of R_2 , so we can assume that the angle of the pile remains unchanged from its initial value. Then we replace $\theta(x,t)$ in (32) by $\theta(x)$ given by the steady-state solution (21), and we arrive to the following equation:

$$\frac{\partial R_2(x,t)}{\partial t} = -v \frac{\partial R_2}{\partial x} - \left(\gamma\delta + \frac{v+v'}{\ell-x} \right) R_2(x,t), \quad (33)$$

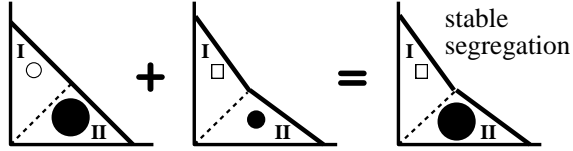
where $v' \equiv \psi\gamma_{21}LR_2^0/R^0$, and $\ell \equiv L(R_1^0 + R_2^0\gamma_{21}/\gamma)/R^0$. The solution of (33) is

$$R_2(x,t) = (\ell-x)^\omega e^{-\gamma\delta t}, \quad (34)$$

with $\omega \equiv (v+v')/v$.

According to the exponential factor $e^{-\gamma\delta t}$ in (34), $R_2(x, t)$ decreases as a function of time when $\delta > 0$. This implies that more large grains are captured, and the perturbation of large grains evolves into the first sublayer of large grains and then to stratification according to the experimental findings [22]. On the other hand, when $\delta < 0$, $R_2(x, t)$ increases as a function of time, so that the large grains of the initial perturbation are amplified, the perturbation disappears, and the segregation profile remains stable.

(a) $\delta < 0$: Grains I : small and cubic (empty)
Grains II: large and rounded (solid)



(b) $\delta > 0$: Grains I : small and rounded (empty)
Grains II: large and cubic (solid)

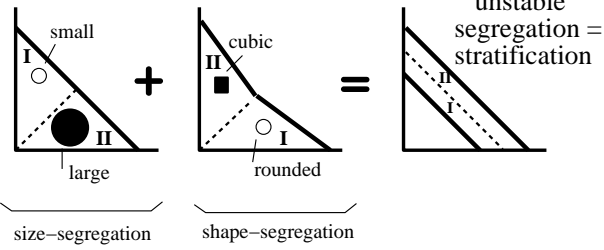


FIG. 7. The instability mechanism for stratification is a result of two competing segregation effects. Size-segregation (first panels in **a** and **b**), and Shape-segregation (second panels in **a** and **b**). **a**, Stable segregation when the mixture is composed of small-cubic grains and large-rounded grains, and **b**, unstable segregation leading to stratification when the mixture is composed of small-rounded grains and large-cubic grains.

V. STRATIFICATION INSTABILITY

The steady-state solution calculated in Sec. III shows the size-segregation of the mixture, while the stability analysis of Sec. IV shows that the grains also shape-segregate according to the value of δ . The stable steady-state solution is achieved when the mixture is composed of small-cubic grains (Grains I in Fig. 7a) and large-rounded grains (Grains II in Fig. 7a). In this case, the segregation of the mixture results because size and shape-segregation act simultaneously to segregate the large-rounded grains at the bottom and the small-cubic grains at the top. On the other hand, when pouring a mix-

ture of small-rounded grains (Grains I in Fig. 7b) and large-cubic grains (grains II in Fig. 7b) an instability develops since the size-segregation and shape-segregation mechanisms tend to segregate the same grain in opposite regions of the cell.

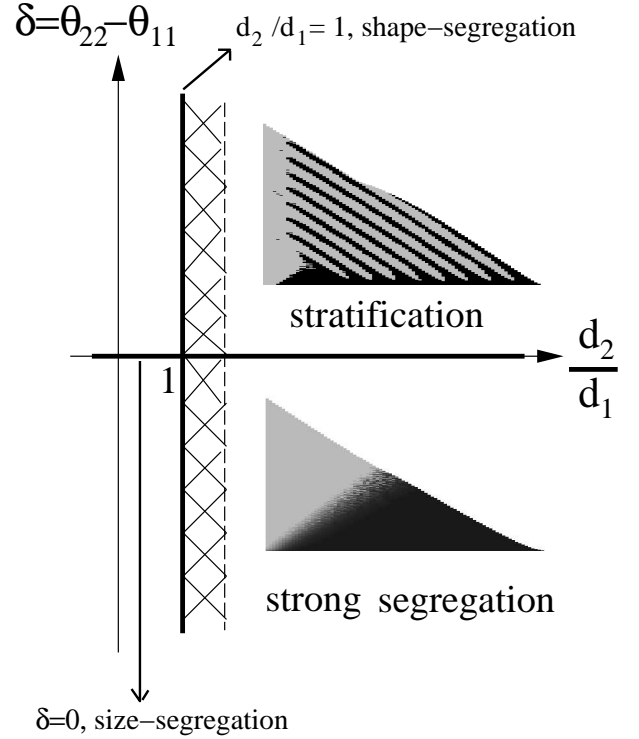


FIG. 8. Phase diagram for two-dimensional flows of granular mixtures. d_2 is the size of the large grains, d_1 is the size of the small grains, θ_{22} is the repose angle of the large grains, and θ_{11} is the repose angle of the small grains. We distinguish the regions of stratification and strong segregation (as shown by the steady-state solution presented here). Weak segregation is expected in the shaded region when the size ratio is close to one. This case is discussed in [35].

Qualitatively, the onset of the instability can be seen as follows. If a small amount of large grains is captured near the center of the pile where the angle of the pile is $\theta \simeq \theta_{11}$ (Point A in Fig. 3), then the repose angle for additional large rolling grains is θ_{22} . Thus, if $\theta \simeq \theta_{11} < \theta_{22}$ (Point B in Fig. 3a), more large grains can be trapped (since the angle of the surface is smaller than the repose angle), leading to the first kink of large grains and then to stratification. On the other hand, the perturbation of large grains disappears when $\delta < 0$. Since $\theta \simeq \theta_{11} > \theta_{22}$ (Point C in Fig. 3b), no more large grains are captured, the fluctuation disappears, and the segregation profile remains stable.

In light of these results we propose the phase diagram shown in Fig. 8. The model presented here predicts a region of stratification ($\delta > 0$), and a region of strong seg-

regation ($\delta < 0$) for size ratios not close to one. In Fig. 8 we show the results of numerical integration of the equations of motion using the following parameters: stratification: $\delta = 0.25$, $\psi = 0.3$, $\gamma_{11} = \gamma_{22} = 1$, $\gamma_{12} = \gamma_{21} = 0.1$, $v_1 = v_2 = 1$, $R_1^0 = R_2^0 = 0.5$, and segregation: the same parameters except for $\delta = -0.1$. For other parameters such as $v_1 \neq v_2$, different $\gamma_{\alpha\beta}$, or $\theta_{12} - \theta_{11} \neq \theta_{22} - \theta_{21}$ we obtain similar results. In addition, when the cross-amplification rates $\gamma_{\alpha\beta}$ are of the order of the amplification rates $\gamma_{\alpha\alpha}$ we also find oscillations in the center of the pile which decay exponentially when $\delta < 0$.

VI. DISCUSSION

In summary, we study analytically segregation and stratification in granular mixtures focusing on the instability mechanism for stratification. We find the steady-state solution of the equations of motion which shows strong size-segregation with the small grains located at the top of the pile, and with the large grains located near the bottom of the pile. In the center of the pile we find a region of mixing where the concentration profiles behave exponentially with a characteristic region of mixing given by $v/(\gamma\psi)$. This region can be of the order of 1.5 – 5 cm and is observed experimentally. We also find that the steady-state solution is stable under a perturbation involving large grains trapped at the center-top of the pile, when $\delta < 0$ (corresponding to large grains less faceted than small grains). On the other hand, the steady-state solution is unstable under the same perturbation when $\delta > 0$ (corresponding to large grains more faceted than small grains). The stratification instability is related to the fact that, when $\delta > 0$, there appears a competition between size-segregation and shape-segregation: the large-cubic grains tend to size-segregate at the bottom of the pile, while at the same time, they tend to shape-segregate at the top of the pile. Thus, the segregation solution becomes unstable, and the system evolves spontaneously to stratification.

[1] R. A. Bagnold, *The physics of blown sand and desert dunes* (Chapman and Hall, London, 1941).
 [2] J. L. Borges, *The book of sand* (Emece, Buenos Aires, 1977).
 [3] H. M. Jaeger and S. R. Nagel, *Science* **255**, 1523 (1992).
 [4] H. J. Herrmann, in *Disorder and Granular Media*, (eds. D. Bideau and A. Hansen) (North-Holland, Amsterdam, 1993).
 [5] S. F. Edwards, in *Granular matter: an interdisciplinary approach*, (ed. A. Mehta) 121 (Springer-Verlag, New York, 1994).
 [6] D. E. Wolf, in *Computational physics: Selected methods –*

Simple exercises – Serious applications, (eds. K. H. Hoffmann, and M. Schreiber) (Springer-Verlag, Heidelberg, 1996).
 [7] H. M. Jaeger, S. R. Nagel, and R. P. Behringer, *Rev. Mod. Phys.* **68**, 1259 (1996).
 [8] J. Duran, *Sables, poudres et grains* (Ed. Eyrolles, 1997).
 [9] J. C. Williams, *Powder Technol.* **15**, 245 (1976).
 [10] A. Rosato, K. J. Strandburg, F. Prinz, and R. H. Swendsen, *Phys. Rev. Lett.* **58**, 1038 (1987).
 [11] J. B. Knight, H. M. Jaeger, and S. R. Nagel, *Phys. Rev. Lett.* **70**, 3728 (1993).
 [12] H. K. Pak and R. P. Behringer, *Nature* **371**, 231 (1994).
 [13] O. Zik, D. Levine, S. G. Lipson, S. Shtrikman, and J. Stavans, *Phys. Rev. Lett.* **73**, 644 (1994).
 [14] W. Cooke, S. Warr, J. M. Huntley, and R. C. Ball, *Phys. Rev. E* **53**, 2812 (1996).
 [15] V. Frette and J. Stavans (submitted to *Phys. Rev. E*, 1997).
 [16] R. L. Brown, *J. Inst. Fuel* **13**, 15 (1939);
 [17] R. A. Bagnold, *Proc. R. Soc. London A* **225**, 49 (1954).
 [18] J. C. Williams, *Univ. Sheffield Fuel Soc. J.* **14**, 29 (1963).
 [19] J. A. Drahn and J. Bridgwater, *Powder Technol.* **36**, 39 (1983).
 [20] S. Savage, C. K. K. Lun, *J. Fluid Mech.* **189**, 311 (1988).
 [21] P. Meakin, *Physica A* **163**, 733 (1990).
 [22] H. A. Makse, S. Havlin, P. R. King, and H. E. Stanley, *Nature* **386**, 379 (1997).
 [23] In addition, when the ratio between the size of the grains is close to one, only a weak segregation of the mixture is found no matter the angle of repose of the species [24,25].
 [24] Y. Grasselli and H. J. Herrmann, *Granular Matter J.* (1998)..
 [25] H. A. Makse, R. C. Ball, H. E. Stanley, and S. Warr, *Phys. Rev. E* **58**, 3357 (1998).
 [26] J.-P. Bouchaud, M. E. Cates, J. R. Prakash, and S. F. Edwards, *Phys. Rev. Lett.* **74**, 1982 (1995).
 [27] J.-P. Bouchaud, M. E. Cates, J. R. Prakash, and S. F. Edwards, *J. Phys. I France* **4**, 1383 (1994).
 [28] P.-G. de Gennes, *C. R. Acad. Sci. (Paris)* **321** II, 501 (1995); P.-G. de Gennes, *Granular matter*, Varenna Lectures (1996).
 [29] E. Clément, J. Rajchenbach, and J. Duran, *Europhys. Lett.* **30**, 7 (1995).
 [30] F. Cantelaube, and D. Bideau, *Europhys. Lett.* **30**, 133 (1995).
 [31] T. Bouteux and P.-G. de Gennes, *J. Phys. I France* **6**, 1295 (1996).
 [32] H. A. Makse, P. Cizeau, and H. E. Stanley, *Phys. Rev. Lett.* **78**, 3298 (1997).
 [33] P. Cizeau, H. A. Makse, and H. E. Stanley, (submitted to *Phys. Rev. E*).
 [34] We focus on the case when the difference in size of the species is not too small (i.e. $d_2/d_1 > 1.4$, where d_1 , d_2 are the typical size of the small and large grains). The case $d_2/d_1 < 1.4$ give rise only to segregation [24,25] and is treated in [35].
 [35] T. Bouteux, H. A. Makse, and P.-G. de Gennes, (submitted to *Eur. Phys. J. B*).
 [36] A. Mehta, in *Granular matter: an interdisciplinary approach*, (ed. A. Mehta) (Springer-Verlag, New York,

- 1994).
- [37] R. A. Bagnold, Proc. Roy. Soc. London **A 295**, 219 (1966).
- [38] H. M. Jaeger, C.-H. Liu and S. R. Nagel, Phys. Rev. Lett. **62**, 40 (1989).
- [39] We do not consider exchange processes [31] in the definition of the collision matrix.
- [40] We notice that this term also includes “cross-capture”, since a rolling grain of type α can be captured on a surface of static grains of type β ($\phi_\beta = 1$).
- [41] According to (16), another possible solution when $\theta_2 < \theta < \theta_1$ is obtained when the denominator of (16a) and (16b) is equal to 0, and $\phi_1 \neq 0$, $\phi_2 \neq 0$. But this solution is not physical because, when $\theta > \theta_2$, large grains can only be amplified but not captured, so that $\phi_2 = 0$ is the only possible physical solution.
- [42] Another possible solution is obtained by trying to impose the solution for Region B for all x . Then we do not consider Region A as a possible solution and the constant C is obtained from $R_1(x=0) = R_1^0$. In this case $C = R_1^0/R_2^0$. However, this solution is not physical since it would imply $\phi_1(x=0) > 1$ if $R_1^0/R_2^0 > r/L$.
- [43] This value was obtained for a cell with a gap of 5 mm between the vertical slabs, and pouring a mixture at a rate of 10 cm³/sec.
- [44] We notice that for comparison with experimental results, all the values of the angles appearing in the theory should be replaced by the tangent of the angles (see Eq. 4).

ACKNOWLEDGEMENTS. I would to thank T. Boutreux and P.-G. de Gennes for many illuminating discussions, and also the hospitality of the College de France where this work was done. I also thank P. Cizeau, H. J. Herrmann, H. E. Stanley, and S. Tomassone for stimulating discussions. I also acknowledge financial support from BP.